Novel method to immobilize phosphate in lakes using sediment microbial fuel cells

Haxthausen, Karl Rasmus August; Lu, Xinyu; Zhang, Yifeng; Gosewinkel, Ulrich; Petersen, Dorthe Groth; Marzocchi, Ugo; Brock, Andreas Libonati; Trapp, Stefan

Published in:
Water Research

Link to article, DOI:
10.1016/j.watres.2021.117108

Publication date:
2021

Document Version
Peer reviewed version

Journal Pre-proof

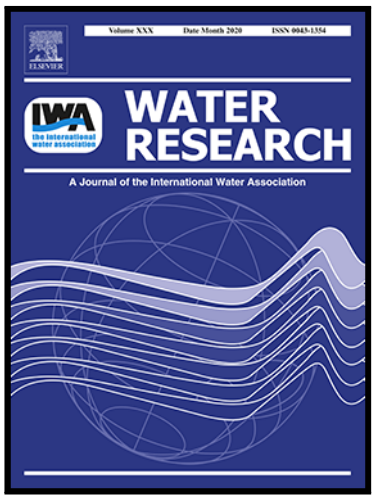

Novel method to immobilize phosphate in lakes using sediment microbial fuel cells

Karl August v. Haxthausen , Xinyu Lu , Yifeng Zhang , Ulrich Gosewinkel , Dorthe Groth Petersen , Ugo Marzocchi , Andreas Libonati Brock , Stefan Trapp

PII: S0043-1354(21)00306-7
DOI: https://doi.org/10.1016/j.watres.2021.117108
Reference: WR 117108

To appear in: *Water Research*

Received date: 25 November 2020
Revised date: 15 March 2021
Accepted date: 31 March 2021

Please cite this article as: Karl August v. Haxthausen , Xinyu Lu , Yifeng Zhang , Ulrich Gosewinkel , Dorthe Groth Petersen , Ugo Marzocchi , Andreas Libonati Brock , Stefan Trapp , Novel method to immobilize phosphate in lakes using sediment microbial fuel cells, *Water Research* (2021), doi: https://doi.org/10.1016/j.watres.2021.117108

Title: **Novel method to immobilize phosphate in lakes using sediment microbial fuel cells**

Authors: Karl August v. Haxthausen[a], Xinyu Lu[a], Yifeng Zhang[a], Ulrich Gosewinkel[b], Dorthe Groth Petersen[c], Ugo Marzocchi[d], Andreas Libonati Brock[a], Stefan Trapp[a,*]

[a] Department of Environmental Engineering, Technical University of Denmark, Bygningstorvet 115, 2800 Kongens Lyngby, Denmark

[b] Department of Environmental Science, Aarhus University, Frederiksborgvej 399, 4000 Roskilde, Denmark

[c] NIRAS A/S, Sortemosevej 19, 3450 Allerød, Denmark

[d] Department of Biology, Center for Water Technology (WATEC) and Center for Electromicrobiology (CEM), Aarhus University, Aarhus, Denmark

*Corresponding author: sttr@env.dtu.dk, telephone: +45 45 25 16 22, fax: +45 4593 2850

Highlights:

- Feasibility of phosphate removal in lakes by sediment microbial fuel cells.
- Efficient phosphate immobilization by steel-mesh electrodes in lab and pilot scale.
- The method was relevant in summer, during anoxia in the hypolimnion.
- Electricity production was insignificant; the focus was on environmental benefits.

Abstract

Phosphate pollution in lakes poses an intractable remediation challenge. Accumulated stocks of phosphorus in sediments cause high concentrations in the overlying water despite elimination of external sources. We propose to use sediment microbial fuel cells (SMFCs) for lake remediation by sediment phosphorus immobilization. The hypothesis is that SMFCs can increase sediment redox potential at the

top layer, and that such changes will allow the sediment to retain phosphorus as immobile species. This study placed an emphasis on scalability, practicality, and use of low-cost materials. Stainless steel net was selected as electrode material, and modifications were tested: (i) chronoamperometric operation with anode poised at +399 mV (versus standard hydrogen potential); (ii) injection of graphite slurry; and (iii) coating with nickel-carbon matrix. Stainless steel electrodes were implemented in laboratory microcosms (1 L) and at field scale in a eutrophic freshwater lake. All tests were carried out in untreated sediment and water from Lake Søllerød, Denmark. Phosphate immobilization was shown at lab scale, with 85% decrease in overlying water using steel electrodes. At field scale maximum phosphate decrease of 94% was achieved in the water body above a 16 m^2 stainless steel SMFC electrode. Results are promising and warrant further study, including remediation trials at full scale. Added benefits include degradation of sediment organic matter and pollutants, inhibition of methane and sulfide emission and production of electricity.

Keywords: Surface water remediation, pilot-scale, in situ, low cost electrode, lake restoration, stainless steel electrode.

Graphical Abstract

see separate file

Competing interests: the authors have no competing interests to declare.

Contributors: all authors have reviewed and approved the manuscript prior to submission.

1 Introduction

For most lakes, phosphorus (P) limits primary production (Stumm and Morgan 1996). High emissions of P into lakes occurred with detergents and raw sewage, during the time when water toilets and sewers were installed but efficient wastewater treatment plants were still lacking. Even though those emissions have been stopped in most Western countries (EEA 2020), the legacy phosphorus now cycles between water columns and sediments of the lakes (Reitzel et al. 2003), with a slow decline in stocks over decades. High phosphate levels initiate eutrophication and algal blooms, with subsequent decreased penetration of light to benthic plants, alteration of predator-prey dynamics and oxygen deficiency. Such ecological modifications have severe consequences for the lakes as habitats, as indigenous species are replaced by a few opportunistic species adapted to such high nutrient and low oxygen levels (Singer 2016). Furthermore, eutrophic lakes lose their value for recreational activities. The problem of eutrophication occurs across all European countries and in all developed countries worldwide. The majority of Danish lakes are eutrophic, based on the indicators: chlorophyll a (70%) and phytoplankton (53%) (Danish EPA 2020).

The sediment represents the major sink of phosphate in lentic systems. With water at oxic conditions, phosphate binds to metals (Fe, Ca, Al) oxides (Nur and Bates 1979; Hansen et al. 2003; Hupfner and Lewandowski 2008) thereby being effectively retained in the surface sediment (Carlton and Wetzel 1988; Shimotori et al. 2019). In lentic waters, prolonged periods of low wind and/or high irradiance typical of summer, may cause water thermal stratification with consequent isolation of the hypolimnion leading to net oxygen consumption in the bottom water (Hupfner and Lewandowski 2008; Giles et al. 2016). Under hypoxic-anoxic conditions, reductive dissolution of iron oxides liberates phosphate which is then released to the water column (Mortimer 1942). The generated ferrous iron (Fe^{2+}) can be effectively scavenged by co-precipitation with H_2S to form Fe-S minerals (Caraco et al. 1993; Roden and Edwards, 1997; Jørgensen, Findlay, and Pellerin 2019), resulting in the net removal of dissolved iron (Figure 1).

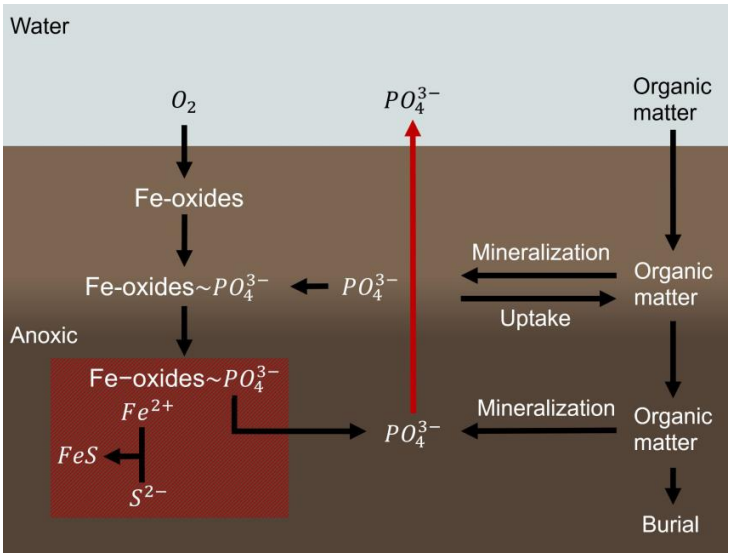

Figure 1. Postulated reactions. Mineralization of organic phosphorous deposited from the water to the sediment produces phosphate (PO_4^{3-}). In oxic sediments matter, iron-oxides are present and bind phosphate. In anoxic sediments (dark brown, bottom), Fe-oxides are reduced liberating Fe^{2+}, which in turn, precipitates with sulfide (S^{2-}) as iron-sulfur minerals (FeS/FeS_2). This reduces the binding capacity of the sediment towards phosphate, that may be then released to the water. By providing an alternative electron sink, the anode of a SMFC inhibits the accumulation of S^{2-} and favors the reoxidation of Fe^{2+} to Fe-oxides thereby maintaining an efficient binding mechanism for phosphate in the sediment (shown in red shading).

Under eutrophic conditions, stimulated primary production in the photic zone enhances the flux of highly degradable organic matter to the hypolimnion, exacerbating O_2 hypoxia. This will in turn increase the release of phosphate from the sediment which will further fuel primary production, leading to a positive feedback loop. Minimizing (ortho-)phosphate release from sediments is a necessary pre-requisite to restore lake water quality to good ecological status.

Aeration of sediments has been applied in lake remediation, but often with limited success (Hansen et al. 2003, Hupfer and Lewandowski 2008, Tammeorg et al. 2020), possibly because oxygen depletion at the sediment-water interface is not the sole driver of phosphate-release from the sediment but also the pH, mineralization of continuously settling organic matter and release of organic-P constitute important

processes (Søndergaard 2007; Hupfer and Lewandowski 2008). We investigate the sediment microbial fuel cell (SMFC), as a tool to promote oxidative reactions in lake sediments with the final aim to limit phosphate release. In a SMFC, the two half reactions (oxidation and reduction) take place at separate electrodes, and the electron transfer is by an electrical current through an external circuit (Logan et al. 2006).

Organic carbon and other reduced species are oxidized by exo-electrogenic bacteria using an electrode (the anode) as electron acceptor and H^+ and CO_2 are produced (Kaur et al. 2014), or spontaneously oxidize on the electrode surface. This reaction is shown in Equation 1, using formaldehyde as a simple example. The electrons released by the oxidation process travel through the external circuit to the opposite electrode (cathode) where they reduce O_2 completing the redox reaction (Equation 2). Thus, the anode facilitates oxidation processes under anoxic conditions using a terminal electron acceptor that can be located at cm to m distance.

Anode reaction: $CH_2O + H_2O \rightarrow CO_2 + 4H^+ + 4e^-$ Equation 1.

Cathode reaction: $O_2 + 4H^+ + 4e^- \rightarrow 2H_2O$ Equation 2.

Studies show that the application of SMFCs favor oxidative processes such as iron and sulfide oxidation in reduced sediment (Tender et al. 2002; Matturro et al. 2017; Touch et al. 2017), with consequent inhibition of Fe-S formation (Ryckelynck et al. 2005), reduced methane emissions (Friedman et al. 2016, Liu et al. 2017) and increased sediment redox potential (Kubota et al. 2019).

The increased availability of ferric iron, induced by the SMFC (with the supply of ferric iron further reinforced by the inhibition of FeS formation), is expected to promote the binding of phosphate to the sediment and thereby limit the lake-internal cycling of phosphate, ultimately reducing the phosphate concentrations in the water column.

The objective of this study was to demonstrate the feasibility of phosphate trapping by installation of SMFCs. Electrodes were tested and optimized in laboratory reactors, and installed in a lake in northern Zealand, Denmark. Over two seasons, electrical, chemical, and biological parameters were monitored.

113 The results of this study may lead to novel surface water remediation techniques, both for natural and
114 anthropogenic systems.

115

116 **2 Materials and Methods**

117 The hypothesis was tested simultaneously in eleven one-liter 2-cell laboratory microcosms (*lab scale*) and
118 in two 4 x 4 m SMFC installations outdoors in a lake (*lake scale*, electrode area multiplied by height of
119 water column gives 112 m^3).

120

121 *2.1 Lake Søllerød*

122 Lake Søllerød is a postglacial lake in the municipality of Rudersdal in Northern Zealand, Denmark
123 (55°48'56.1"N 12°29'33.5"E). Its surface area is 13 ha with a maximum depth of 9.8 m and an average
124 depth of 5.6 m (Jensen and Møller 2015). A thermocline regularly establishes in about 3 m depth in the
125 period May to September. The lake receives water from four rainwater discharge pipes and through a
126 creek (6.6 L/s) dewatering a bog area. The average hydraulic retention time is 5 to 6 years (Jensen et al.
127 2009).

128 Untreated wastewater was emitted into the lake until 1924, whereafter treated wastewater was emitted
129 until 1975. In the 1960's cobber-sulfate was added to limit odors. Another attempt of remediation was
130 pumping of bottom waters, which has been intermittently carried out between 1976 and 2009 (Grontmij,
131 2012). Between 1922 and 1975, averaged concentrations of total P during summer in the epilimnion were
132 above 2500 µg/L. By the end of the 1970s total P steeply declined to values near 100 µg/L in surface
133 samples, but up to 600 µg/L total P was found in the bottom water, most of it in the form of dissolved
134 phosphate, and has since then declined very slowly (Jensen and Møller 2015). In 2018, the maximum
135 concentration of phosphate-P in bottom water from 8 m depth was 962 µg/L (Nicolaisen 2018). The high
136 phosphate levels lead to intense algal growth (though, during summer, nitrogen may become limiting),
137 with Secchi depths often < 1 m and chlorophyll-a over 150 µg/L, and subsequent elevated pH-values up
138 to 10 (Jensen and Møller 2015). Primary production has been high for several decades, resulting in high

sediment biomass (Danish Environmental Ministry 2012, Danish Environmental Ministry 2015). The top sediment layer is black muddy gel-like gyttja of about 50 cm thickness, the underlying layer is more solid silt with gas intrusions and is about 100 cm thick. The total volume of anthropogenically affected sediment has been estimated at 103 025 m^3 (Hvidt 2016). In July 2017, measured concentrations of total P in sediment ranged from 1600 to 3200 mg/kg dry weight (dw). Sediment stocks of P are estimated at 9700 kg in the top 40 cm, of which 50-80% is bound to iron and the remainder mainly bound in organic matter (Jensen et al. 2009), while external P input is only 61.5 kg/year (Danish Environmental Ministry 2012). The lake and lake sediment are well studied. Its location is only 4 km north of the university campus at Kongens Lyngby. Lake Søllerød was thus chosen as field site for the lake scale test of P immobilization using SMFCs.

2.2 Laboratory microcosms (reactors)

Lab-scale SMFCs were constructed from two 650-mL chambers separated by a CMI-7000S cation exchange membrane (Membranes International Inc., USA) with aperture diameter of 70 mm. A two-chamber system with membrane separation was favored over a one-chamber system, to avoid penetration of oxygen through the open water layer to the sediment surface. Oxygen would oxidize the top sediment, allowing phosphate binding and thus mask the effect of the electrode. In field trials the membrane is not necessary, as height and stratification of the water column limit oxygen diffusion. The microcosm design is shown in Figure 2. The reactor walls were manufactured from transparent acrylic plate and tubing, O-rings were made of nitrile rubber, stoppers of natural rubber, gaskets of soft PCV, washers of brass, and rods and wingnuts of AISI304 stainless steel. Access ports to each chamber were closed with rubber stoppers and generously sealed with petroleum jelly (Vaseline) to prevent oxygen intrusion. Petroleum jelly was also applied on the anode chamber exterior at connecting joints. Electrodes were placed 15 mm from the membrane.

The lab scale experiments were conducted using sediment and water collected in one batch from Lake Søllerød. Samples were sieved to remove debris larger than 10x10 mm, and sediment (anode chamber, 60%) and water (anode chamber 40% and cathode chamber 100%) were added without further pre-

166 treatment. Reactors were operated at room temperature (range 19 to 26 °C) and in the dark, to avoid
167 potential photosynthesis and oxygen formation.

168

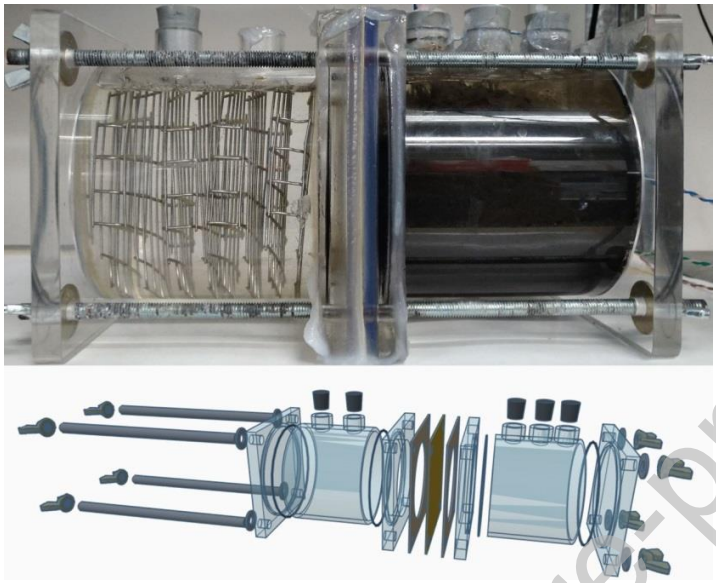

169

170 **Figure 2.** Laboratory microcosms (reactors). Top: operating microcosm containing lake water in the
171 cathode chamber (left), and lake sediment and water in the anode chamber (right). Cathode and anode
172 were made of stainless steel, folded to extend throughout their respective chambers. Bottom: external
173 components of the microcosm. Elements left to right: wing nuts, tensioning rods, disk washers, end plate,
174 O-ring, cathode chamber and stoppers, O-ring, interface plate, gasket, membrane, gasket, interface plate,
175 O-ring, anode chamber and stoppers, end plate, disk washers, and wingnuts.

176

177 *2.3 Test of electrode materials*

178 Anode and cathode were in all cases constructed from the same material to prevent interference from
179 galvanic corrosion. Electrodes with specific surface area of 0.0023 m^2, were cut from 1 mm diameter
180 AISI316 stainless steel wire spot-welded in 10-by-10-mm squares, and folded to distribute electrode
181 layers evenly in each reactor chamber. Various electrode configurations were tested at laboratory scale: i)
182 blank stainless steel electrodes (steel); ii) graphite slurry (graphite) injected as a means of increasing the

183 effective anode surface area and the range of a standard steel electrode. The graphite slurry consisted of
184 25 g pulverized graphite suspended in 50 mL lake water and was injected into the sediment in the anode
185 chamber. iii) A coating of nickel-doped carbon (Ni-C) was tested as surface treatment, potentially
186 leveraging carbon's affinity for biofilm adhesion (Logan 2008) and nickel's catalytic properties (Choi 2019,
187 Gupta 2017). Ni-C electrodes were electrolytically coated in a carbon and nickel solution, embedding
188 nickel particles in a carbon matrix. iv) Chronoamperometric operation was carried out using a potentiostat
189 (Pot16, ACM instruments, UK), poising steel anodes at +200 mV *vs.* an Ag/AgCl electrode (4 M KCl gel,
190 Equilibrium, France; potential against standard hydrogen electrode SHE is +399 mV) (poised). v) The
191 control employed disconnected steel electrodes (DCtrl), to determine any effect inherent to the presence
192 of steel. vi) A second type of controls (Ctrl) was constructed by simply omitting electrodes. Each type of
193 reactor was run in duplicate, except DCtrl which was only one reactor.

194 The performance of SMFCs was determined by measuring working potential (WP, in mV) and open circuit
195 potential (OCP, in mV). The flow of electrons (unit A·s, Ampere seconds, or Coulomb C) was calculated
196 from WP and external resistance and subsequently used for stoichiometric calculations of substrate
197 oxidation (1 mol e^- is equivalent to 96 485.33 A·s) (Logan et al. 2006). The external resistance (between
198 anode and cathode) was 1000 Ω until day 24 and 200 Ω from then on, except for the Ni-C electrode,
199 where the resistor was changed after 140 d.

200 In microcosm experiments, WP was measured hourly using a data logger (CR1000, Campbell Scientific).
201 The OCP was determined only at the control reactors with disconnected electrodes (DCtrl) to avoid
202 disturbance of the microbial community.

203

204 *2.4 Lake installations*

205 The first SMFC was installed in the lake in July 2019, the second in June 2020, and both are still in
206 operation at the time of writing (November 2020). The construction and installation is shown in Figure 3.
207 Steel wire mesh (as described previously) was suspended in 4 x 4 m frames made from heavy duty PVC
208 tubing. Anodes were made by three layers of steel, cathodes by one layer only. Initially, anode frames

were filled with air. When in place at the lake, upon removal of rubber stoppers they filled with water and sunk to the bottom. Frames would settle a few centimeters into the sediment, placing the anode steel layers just at the surface of the sediment but avoid sinking into the sediment. Cathodes were constructed with buoyant internal chambers to achieve 5 kg negative buoyancy. Anodes and cathodes were tethered in their corners in the desired anode-cathode distance, and swimming marking buoys were connected to the four corners using ropes. Electrical wires robustly connected to each electrode were accessible from a utility box placed on the nearest bank. The first field (Field 1) was constructed with a fixed distance between anode and cathode of 3 m, the second field (Field 2) was constructed with adjustable anode-cathode distance, and the cathode was adjusted to 1.5 m depth below water surface. Electrodes were assembled on shore, and then towed in position and sunk, anode Field 1 at 4 m depth (from May 2020 7 m depth) and anode Field 2 at 7 m depth.

Figure 3. Installation of electrodes in the lake. Anode was folded (A), electrodes were installed in frames and towed in position (B). Electrodes were sunk. Cathode was suspended between surface buoys and the anode on the bottom (C), performance was monitored by measuring working potential on shore (D).

2.5 Chemical analysis

During lab scale experiments, water samples were collected from the anode chamber by inserting a syringe needle through the rubber stoppers. Due to low operating volume and the desire to limit possible disturbances, only 3 rounds of sampling were carried out. During lake scale experiments, water samples were collected from the top, middle and bottom of the water column above the anode and nearby at a control site, using Teflon tubing and a peristaltic pump from a boat. Sampling at high wind speed was avoided, to circumvent mixing of the water close to the electrode with surrounding lake water but also for safety reasons. All water samples were measured immediately for dissolved oxygen (DO), pH, electrical conductivity (EC), and temperature with hand-held electrodes (Wissenschaftlich-Technische Werkstätten Weilheim WTWW). Additional water samples were passed through 0.2-µm nylon filters and stored at –20 °C until analysis. Inorganic N and P (NH_3-N, NO_2-N, NO_x-N, and PO_4-P) were analyzed using a SKALAR San++ continuous (segmented) flow analyzer. Elemental analysis was done using Inductive Coupled Plasma with an Optical Emission Spectrometer (ICP-OES, Perkin Elmer Avio 200) or to a Mass Spectrometer (ICP-MS, Agilent 7700 Series) equipped with Syngistic™ for ICP Software v. 2.0 from Perkin Elmer. Sediment samples were centrifuged in 15-mL vials at 8800 x g for 10 minutes, freeze-dried, and digested in microwave oven (USEPA 3051A method) with 9 mL HNO_3 (65%), 3 mL HCl (30%) and 1 mL H_2O_2 (30%). Pore-water samples were taken from the supernatant of the centrifuged sediments.

2.6 Statistical analysis

The difference in the median values of measured PO_4-P concentrations above the electrode versus those at the control site was tested by the Mann-Whitney U-test (with significance level 5%) in the SPSS 22.0 software. Other differences in mean were tested using the two-sided t-test in MS Excel 2010.

3 Results

3.1 Laboratory microcosms

Figure 4 summarizes the performance of the SMFCs at lab scale. Within a few days the OCP of the disconnected control (DCtrl) reached 650 mV and remained constant above 600 mV until day 130, then slowly increased to 885 mV at the end. This OCP confirmed the well-functioning of the system, the absence of significant oxygen intrusion, and ongoing reduction processes in the untreated sediment. Measured working potentials of the steel and the graphite electrodes showed little difference, with an initial rapid increase to values > 100 mV, and at day 24, when the resistance was lowered from 1000 Ω to 200 Ω, a decline to about 40 mV, then constant until day 170, from then on instable and circulating. We suspect that from day 170 on the reactors were no longer fully operating.

The highest WP was seen for the Ni-C electrode, which was started 64 days after the other electrodes. It quickly reached 600 mV after a few days, but from then on slowly declined over 140 days. Day 204, the resistance of the Ni-C reactor was changed from 1000 Ω to 200 Ω, and the WP fell accordingly by factor five to values lower than those measured for the other electrodes. However, the nickel electrode corroded and formed nickel(II)phosphate (see section 4.6).

Initial PO_4-P concentrations taken a few days after filling the reactors (immediate sampling was prohibited by particle resuspension) were between 2500 and 3500 µg P/L for all samples, except in the reactor with Ni-C electrodes, P concentrations were very low (< 1 µg/L) from the start to the end of the experiment. At day 134, half-way through the experimental period, measured PO_4-P had fallen in the steel and graphite reactors to about 500 µg P/L, while in the controls an increase to > 4000 µg P/L was observed. Between day 134 and 217 (end of experiment), phosphate increased in steel, graphite, control, and DCtrl microcosms. At the end of the experiment, PO_4-P was 7020 and 6969 µg/L in Ctrl and DCtrl, respectively, 2663 µg/L with steel and 2198 µg/L with graphite electrodes. Poised reactors showed continuously decreasing phosphate, and Ni-C reactors exhibited consistently low phosphate concentration with maximum 41 µg/L. The variation of the measured values was small for samples taken from the steel and

273 graphite test initially and at t = 134 d, but towards the end, the WP got instable, and also the variation of
274 measured P was large, hence those final values should be interpreted cautiously.

275

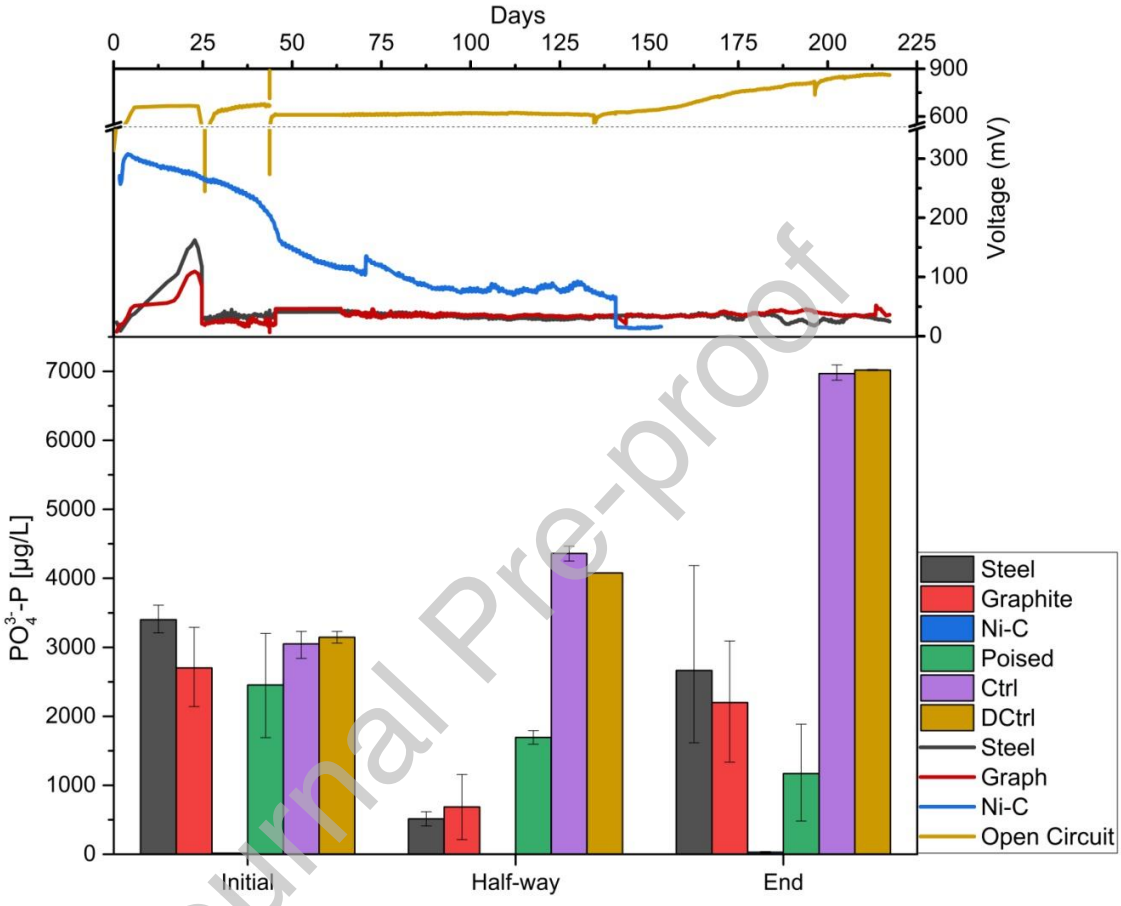

276

277 **Figure 4.** Results from lab scale experiment. Top: open circuit potential (OCP, mV, right axis) and
278 working potentials (mV, right axis, mean of two replicates), below: dissolved phosphate in the water
279 column PO_4-P (µg/L, left axis, error bars denote minimum and maximum, number of replicates n is 2 to 4)
280 at initial (day 0), half-way (day 134) and at the end (day 217). Electrode materials: stainless steel (Steel),
281 stainless steel with addition of graphite particles (Graph), stainless steel coated with carbon embedded
282 with nickel particles (Ni-C), stainless steel with external voltage applied (Poised), no electrode (Ctrl), and
283 disconnected steel electrodes (DCtrl).

284

285 In Figure 5 total phosphorus (TP, mg/L) and total iron (TFe, µg/L) in pore water and water column at the
286 end of the experiment, day 217, are shown. All SMFC-treated reactors showed lower concentrations of
287 TP and TFe in pore water and water column than Ctrl and DCtrl. This supports the hypothesis that
288 phosphate is eliminated by co-precipitation with iron in reactors with connected electrodes. Moreover,
289 TFe is always below TP (note the different axes), giving iron the limiting role. An exception is the Ni-C
290 reactor, where measured TP in the water column was low despite relatively high TFe. As reduced Fe^{2+} is
291 soluble, but oxidized Fe^{3+} is not, this could be an indication that SMFCs affect the oxidation status of iron.
292 TFe was only assessed when the reactors were sacrificed at the conclusion of the experiment, hence the
293 data reflects the situation after the reactors showed instability. It is possible that the TFe concentrations
294 were lower at day 134, when also lower PO_4-P concentrations were seen (compare Figure 4). TP values
295 are similar to (Ctrl, DCtrl) or higher (steel, graphite, poised) than those for PO_4-P shown in Figure 4, the
296 latter indicating the occurrence of other forms of P, probably organic P. A plausible source of organic P is
297 the partial microbial decomposition of sediment material, which is stimulated by the electrodes.

298 No significant difference between the treatments could be observed for TFe and TP in sediment solid
299 samples (not shown). The mean sediment content of TFe was 9058 mg/kg dw (standard deviation *s* 1495
300 mg/kg dw, *n* = 24), of Al was 4888 mg/kg dw (*s* 992 mg/kg dw, *n* = 24), while that of P was 966 mg/kg dw
301 (*s* 270.2 mg/kg dw, *n* = 24). The analysis of heavy metals showed moderate pollution with Cu (mean 470
302 mg/kg dw, *s* 68.9 mg/kg, *n* = 24) and lead (mean 85.4 mg/kg dw, *s* 16.1 mg/kg dw, *n* = 24). The rank
303 correlation between TP in water column and sediment (not shown) was significant ($r = 0.50$, $n = 24$,
304 significant at $P = 0.05$) but the explained variance is low ($R^2 = 0.26$), while the relation between P in
305 sediment and in pore water was below significance ($R^2 = 0.13$, $n = 16$).

306 The concentration of Ni in all sediments was low, 13.4 mg/kg dw on average (*s* 2.8 mg/kg, *n* = 21), with
307 the strong exception of the sediment treated with the Ni-C electrode. Here, the mean was 4767 mg Ni/kg
308 dw (*s* 1108 mg/kg dw, *n* = 3). Additionally, very high concentrations of dissolved Ni in pore water (17.5
309 mg/L) and water column (40 mg/L) were measured (all other water samples: 1 to 7 µg/L) in the Ni-C
310 samples, and also Co was elevated (17 µg/L in pore water and 43 µ/L in overlying water, all other

311 samples < 1 µg/L). The concentration of Cr in solid samples was on average 19.8 mg/kg dw (*s* 3.0 mg/kg
312 dw, *n* = 18), and slightly elevated in samples with poised electrodes (mean 22.5 mg/kg dw, *n* = 6,
313 significantly different in a two-sided t-test, *P* = 0.03). However, no difference was observed for the water
314 samples (mean of samples from poised reactors: 2.8 µg/L versus 3.1 µg/L, mean from all other reactors).

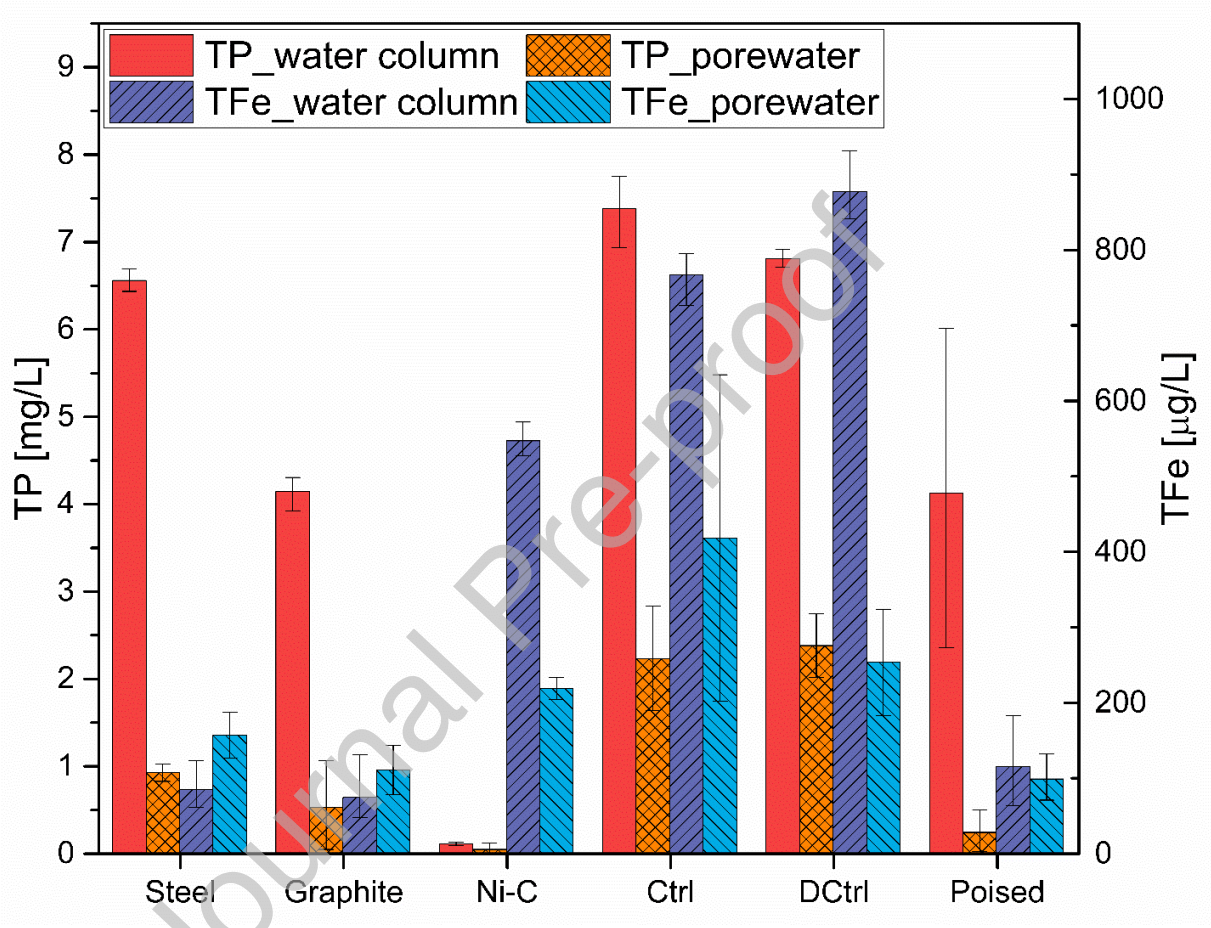

315

316 **Figure 5.** Total phosphorus (TP, mg/L, left axis) and total iron (TFe, µg/L, right axis) in sediment pore
317 water and in the water column of microcosms with and without sediment microbial fuel cells, at the
318 termination of the lab scale experiments on day 217. Error bars denote minimum to maximum, *n* is 2 to 6.
319 Electrode materials: stainless steel (Steel), stainless steel with addition of graphite particles (Graphite),
320 stainless steel coated with carbon embedded with nickel particles (Ni-C), stainless steel with external
321 voltage applied (Poised), no electrode (Ctrl), disconnected steel electrodes (DCtrl).

322

3.2 Lake installations

Results for the lake installation are presented in Figure 6. The electrical charge (cumulative Ampere, As) shows a strong seasonal pattern, with the highest slope (and thus highest electrical current) during summer months, Field 2 also in early autumn 2020. The phosphate concentrations were significantly lower in samples taken in the proximity of the anode, compared to controls (two-sided U-test, $P = 0.00$). In late spring 2020, intense phosphate release was observed in the lake. In the controls, the increase in PO_4-P continued into summer and reached values > 800 µg/L. However, concentrations as low as 41 µg/L (6% of the control at 653 µg/L) were observed above the anodes during July 2020. The rapid drop in phosphate concentration was paralleled by a sharp increase of SMFC performance, measured as cumulative ampere (Figure 6). Field 1 generated a maximum of 10 mW, causing high initial cumulative ampere, although plateauing after one month, and low or no electrical current during winter. The electrode field was towed ashore for inspection in May 2020 (day 300). A ripped cable was found, and repaired, after which the electrodes were moved to deeper waters (7 m) and re-installed.

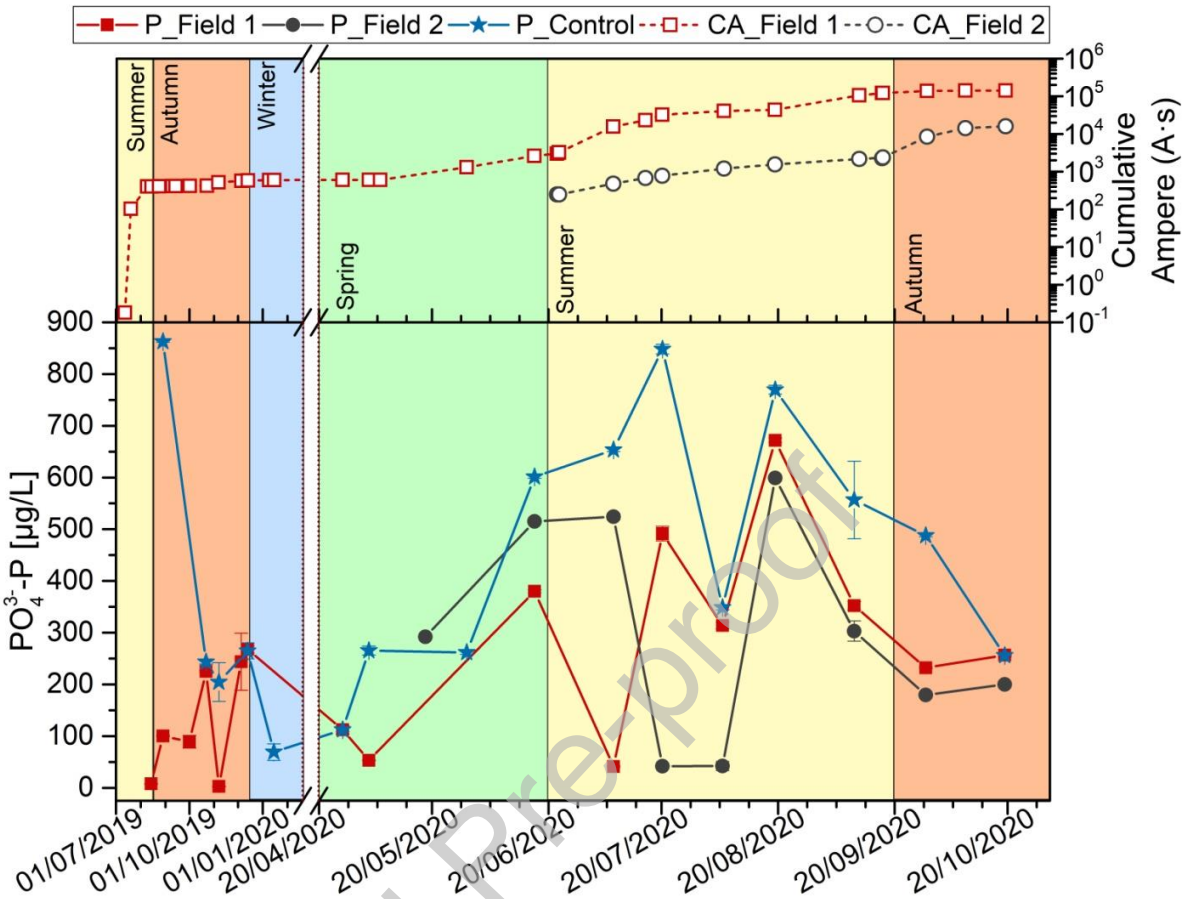

336

337 **Figure 6.** Lake scale sediment microbial fuel cell performance. Cumulative ampere (A·s) generated by the
338 electrodes of Field 1 and Field 2, and PO_4-P concentrations (µg/L) measured at the bottom of the lake
339 water column above the anodes and at a control site. Error bars denote standard deviation. The cable to
340 the anode of Field 1 was broken from January to May 20th, 2020, indicated by the broken x-axis.

341

342 The generated current of both electrodes was decreased when oxygen in bottom waters was high (Figure
343 7, spring and autumn). In summer 2019, a thermocline with low DO at depths ≥ 3 m was observed, but
344 was disturbed by stormy weather in mid-August. In summer 2020, a stable thermocline developed from
345 May and lasted into late September (Figure 7, 21 July to 11 September). The current generated in the
346 SMFCs and the phosphate measured near the lake bottom were likewise low during winter, with little
347 difference between electrode and control, which can be contributed to the naturally aerated bottom waters

348 in that period. With increasing temperature during summer, the electrode performance increased. In
349 parallel, P concentrations increased, the increase being less at the anodes than the control.

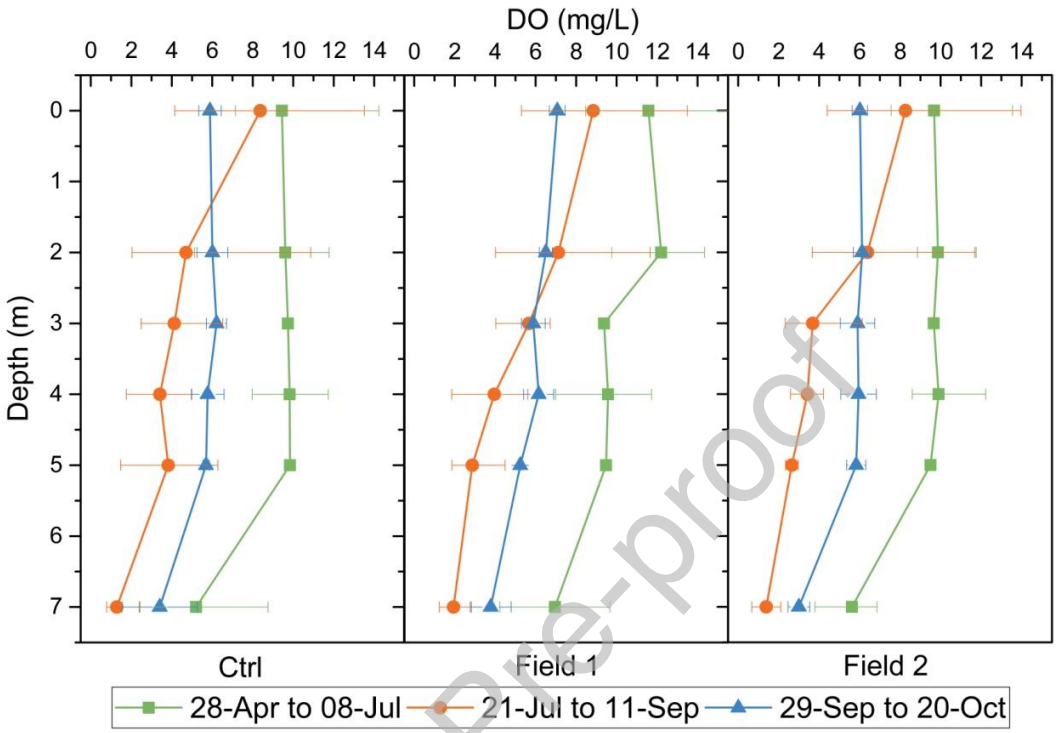

350

351 **Figure 7 Dissolved oxygen versus depth for control field, Field1 and Field 2**. Dissolved oxygen
352 (mg/L) measured in the lake water column at varying depth. Symbols denote median, error bars are
353 minimum and maximum of n is 5 (28-Apr to 08-Jul), 4 (21-Jul to 11-Sep) and 2 (29-Sep to 20-Oct).

354

355 **4. Discussion**

356 The underlying hypothesis of the experiments was that by increasing the redox potential of the sediment
357 top layer with an SMFC, phosphate would be eliminated from the lake water. This hypothesis was tested
358 at lab scale and at lake scale.

359

360 *4.1 Lab Scale*

361 At lab scale, phosphate concentrations were significantly reduced in all SMFC reactors at t = 134 d. No
362 effect was observed from the presence of disconnected steel electrodes, as DCtrl differed little from the
363 controls without electrodes (Figure 4). No additional effect was observed from addition of graphite slurry:
364 cumulative ampere and P concentrations were similar for the reactors with graphite and steel electrodes
365 (Figure 4).

366 Given that the volume ratio sediment to water was 3:2 in the laboratory reactors, and that indoor
367 temperatures higher than those at the bottom of the lake stimulate microbial processes and thus the
368 release of phosphate from sediment, the experiment can be considered worst-case. Nonetheless, we
369 documented partial elimination of P from the water phase. Compared to the initial concentrations
370 measured in the water column, the decrease of PO_4-P at day 134 was 85%, 75%, and 31% for the steel,
371 graphite, and poised reactors, respectively, while for Ctrl and DCtrl, the PO_4-P increased by 43% and
372 30%.

373

374 *4.2 Lake Scale*To quantify the effects of the SMFCs, water samples were collected near the center of the
375 anode. This sampling method would probably fail when bottom water is not stagnant and mixing with the
376 surrounding water occurs. Mixing can be induced by heavy winds, in particular at times with non-
377 established thermocline from autumn to spring. In this period, no difference in phosphate concentrations
378 between controls and test fields could be found (Figure 6). However, in this period also oxygen was
379 present at the bottom (Figure 7), and oxidation of the top sediment layer could have masked the effects of
380 the electrodes. With warmer weather, the lake became stratified, which is reflected in the depth profile of
381 DO (Figure 7): during summer (21 July to 11 September), stratification was evident and DO was low
382 below 3 m depth. Concomitantly, the PO_4-P concentration normally decreases during winter and early
383 spring in nutrient rich Danish lakes (Søndergaard et al. 2005). With increasing temperatures, faster
384 decomposition of sedimented organic matter and a higher rate of diffusion from sediment to water column
385 led to increasing release of PO_4-P (Jensen and Andersen 1992; Boström et al. 1982; Gomez et al. 1998;
386 Søndergaard 2007). The same happened in Lake Søllerød, with a steady increase of PO_4-P
387 concentrations from April to July 2020, stable at the end of July, while an algal bloom occurred, and

388 decline from August to October. This trend occurred both for controls and test fields, but with reduced
389 PO_4-P at the test fields.

390 The electrical charge delivered by the electrodes, but not the release of P, was inversely linked to DO at
391 the bottom of the water column. In periods with oxygenated hypolimnion, PO_4-P concentrations in control
392 samples fell to low values, similar to those near the treatments at Field 1 and 2. This was both observed
393 in autumn and winter 2019, and at the last measurement 20th October 2020. Hence, P immobilization
394 continues when the bottom water becomes oxygenated, but since it was measured both for control site
395 and test fields this must be contributed to the oxygenation and not to the effect of the electrodes. The
396 electrodes become effective during summer and until early autumn, when the bottom water is low in
397 oxygen (also seen from the electrical current, Figure 6). As oxygen depletion increased with depth, the
398 SMFC Field 1 was relocated in May 2020 to deeper water (from 4 m to 7 m depth).

399

400 *4.3 Mechanism*

401 A plausible underlying mechanism for the decrease of P is that iron-oxides (e.g. FeOOH), as produced by
402 the oxidation of ferrous iron at the anode, efficiently bind phosphate, thereby preventing/minimizing its
403 efflux from sediment to water (Roden and Edmonds 1997; Hansen et al. 2003; Lehtoranta and Pitkänen
404 2003). Under reducing conditions, such as the one expected in our untreated lake sediment (Jørgensen,
405 Gabriel and Boock 2000), iron and sulfur are reduced to Fe^{2+} and S^{2-} and co-precipitate as FeS, with
406 phosphate being released into the water. The accumulation of FeS minerals is visible from the black color
407 of the sediment (Jensen and Andersen 1992). A change of color from black to grey, was visible by eye in
408 the surroundings of some electrodes (< 1 mm distance), suggestive of net depletion of FeS minerals. The
409 ability of SMFCs to decrease the amount of hydrogen sulfide (H_2S) produced in the sediment has been
410 shown (Ryckelynck et al. 2005; Touch et al. 2017; Kubota et al. 2019; Algar et al 2020). Elimination of
411 sulfide inhibits binding of iron as FeS and FeS_2 (Søndergaard 2007), thus increasing the pool of dissolved
412 iron available for anodic oxidation. Inhibition of P efflux as observed in our experiment can thus be
413 explained in the context of previous literature showing a shift of the redox state of iron that ultimately favor
414 P trapping in iron(III) minerals. Cable bacteria, electrically conductive filamentous *Desulfobulbaceae*, may

produce analogous effect (*i.e.*, increase the sediment redox potential and favor P immobilization via promoting FeS dissolution (Marzocchi et al. 2020; Sulu-Gambari et al. 2016). However, amplicon sequencing of the variable regions V3 and V4 of the bacterial 16S rRNA gene did not identify cable bacteria in sediment samples from neither laboratory nor lake installations (data unpublished), further supporting the link between SMFC treatments and observed decrease in phosphate.

4.4 Mass balance

Measured sediment TP concentrations were close to 1000 mg/kg, while P concentrations in lake water rarely reached 1 mg/L, most of the time much less (Figure 6). Hence, the top cm of sediment contains more P than the whole water column. It is thus meaningless to place the electrode deep within the sediment, even though this may lead to a higher yield of electrical charge, because release of P from the top sediment is sufficient to eutrophicate the whole lake. Regardless, a complete oxidation of sediment (thickness up to 1.5 m, (Jensen et al. 2009)) cannot be achieved in reasonable time periods. Moreover, upon decomposition of the sediment, all nutrients and pollutants stored over decades would be released, with possibly unfavorable outcome for water quality and lake ecosystem. The goal was therefore, to establish a barrier within the top of the sediment by creating an oxidized layer that prevents the escape of P from decomposition of organic matter buried in the sediment. Consequently, the anode was designed to be placed within and on top of the sediment. As new organic matter (from dead algae and detritus) settles over the year, the anode needs a certain thickness. This was achieved by creating a stacked electrode of three layers.

4.5 Microbial Turnover to Electrons (MTE)

The total amount of electrons produced in the laboratory steel and graphite reactors over the full experimental period was similar, about 3000 As, corresponding to 31.1 mmol e^-. The peak power production of the lake electrodes was 10.5 mW (324 mV at 10 Ohm). This is comparable to earlier power achievements with freshwater SMFCs (De Schamphelaire et al. 2008), but not an efficient electrical

power source. Thus, the benefit of the lake SMFCs is not electricity production, but improvement of the lake environment. The electrode in Field 1 produced more than 100 000 A·s over its lifetime of 15 months, or 1.04 mol e^-. Two mol electrons correspond to the reduction of one mol elemental S to H_2S, and four mol to the reduction of one mol C to CH_4. Thus, a calculated 518 mmol (18.7 g) H_2S were not formed. Sulfide is very toxic to higher life, such as fish, and it binds iron, thus prohibits binding of P, which is the main reason for eutrophication. The electrons produced also correspond to 260 mmol methane (4.15 g CH_4). Calculated for the whole lake area (13 ha), 539 kg CH_4 could have been avoided. In fact, lake sediments are among the most important natural methane sources on a global scale (Bastviken et al. 2004). De Schamphelaire et al. (2008) list as other potentially beneficial effects of SMFCs the avoidance of toxic mercury and arsenic species formation. Moreover, the degradation of petroleum hydrocarbons by SMFCs has previously been documented (Marzocchi et al. 2020). In the lab scale reactors, we also observed a significant reduction of dissolved lead (Pb) in pore water and overlying water (mean 4.2 µg Pb/L in Ctrl and DCtrl, n = 10 to < 0.5 µg Pb/L in reactors with MFC, n = 30, significant at $P < 0.05$), while no significant difference was found for Cu, Zn and As.

4.6 Corrosion resistance and long-term stability

The anodes placed in the top of the lake sediment showed no sign of corrosion, while the cathodes were overgrown by periphyton with time. This reduced the performance of the whole system, as will be described later (Haxthausen 2021, in prep.). The steel electrodes were made of Stainless Steel 316, which has superior corrosion resistance (ESPI Metals 2020). The alloy contains 12% Ni and 17% Cr (and 0.45% P). No elevated levels of these heavy metals were observed in water or sediment treated with steel electrodes. However, slightly elevated levels of Cr were observed in sediments (though, not in water) treated at lab scale with electrodes poised by a constant potential of +400 mV vs. SHE. It may be concluded that the constant flow of electrons to keep the potential high supports the corrosion of Steel 316.

A drastic increase of Ni in sediment and water samples from microcosms treated with Ni-C coated electrodes was observed. These elevated levels of Ni obviously originate from the nickel. Ni can react

468 with phosphate and form insoluble nickel(II)phosphate ($Ni_3(PO_4)_2$) giving off a green color that was in fact
469 visible. The constant and very low PO_4-P concentration observed in the Ni-C treated reactor is hence very
470 likely caused by Ni dissolution from the electrode. The concentration of TFe in both water column and
471 pore water in the Ni-C reactors exceeded that of all other treatments, further indicating that the decrease
472 in PO_4-P was not exclusively related to precipitation with Fe (Figure 5). The high toxicity of nickel to
473 aquatic organisms (predicted environmental no effect concentration PNEC is at 7.1 µg/L (ECHA 2020),
474 while the concentration of Ni in the headspace water was 40 mg/L) prevents the use of this type of Ni-C
475 coated electrodes in open freshwater ecosystems.

476 In the lab reactors with steel and graphite electrodes, the measured working potential became instable
477 after day 170 and showed cycling values (Figure 4). This instability may have been caused by fouling of
478 the electrodes or by a malfunctioning of the membrane between anode and cathode chamber. An
479 increase of PO_4-P in these reactors was observed at the final measurement, accompanied by a decrease
480 in the NO_X-N concentration (not shown). This may indicate that the redox potential in the anode chamber
481 decreased (became more negative), and nitrate became a favorable electron acceptor. Nitrate creates a
482 redox potential high enough to sustain iron in an oxidized form and thus impacts the redox-dependent
483 retention of phosphorus (McAuliffe et al. 1998; Duras & Hejzlar 2001, Jensen and Andersen 1992). A
484 concomitant increase in NH_3 was also observed (data not shown), likely related to oxidation of organic
485 matter. Some effect can be ascribed to the increase in temperature (day 217 corresponds to 7th of July
486 2020), since the concentration of PO_4-P and NH_3 also increased in the poised reactors.

487

488 *4.7 Comparison to other findings*

489 A similar effect of SMFC on phosphate and iron concentrations has been observed in lab-scale marine
490 systems using carbon cloth as anode material (Touch et al. 2017). In that study, the decrease in pH led to
491 release of Fe^{3+} and concomitant removal of phosphate. In a laboratory study, Yang et al. (2016) observed
492 binding of phosphate spiked to the water phase from overlying water of a SMFC containing lake
493 sediment. Within 30 days, concentration of P in the water column fell from 0.1 mg/L to 0.01 mg/L in the
494 SMFC-treated system, but remained almost constant in the control. Different from our study, the authors

used open 2 L glass beakers without membrane. A similar set-up with the Søllerød lake sediment in our laboratories was unsuccessful because the sediment top layer was oxidized and P was bound to sediment both in controls and SMFC-treated replicates (Nicolaisen 2018).

Previous research conducted in 15 Danish lakes showed that when the sediment TFe:TP (w/w) ratio exceeds 15, phosphate release from the sediment under oxidized conditions is low (Jensen *et al.* 1992; Søndergaard 2007). The measured ratio for the sediment used in the SMFC reactors was 9058 mg TFe/kg dw to 966 mg TP/kg dw, or 9.4 to 1, hence below this threshold. However, there were also 4888 mg Al/kg dw present, which also can adsorb P (Hansen et al. 2003). In earlier studies of Lake Søllerød, Jensen et al. (2009) found a less favorable ratio of TFe:TP ≤ 7. Restoration of the lake by addition of aluminum salts $Al(OH)_3$ for P co-precipitation was discussed, but dismissed due to the occasionally rather high pH levels, which can effect dissolution of aluminum salts and Al toxicity in the lake ecosystem (Jensen et al. 2009, Gensemer and Playle 1999).

4.8 Safety

The Ni-C electrodes, which released large amounts of nickel, and the poised electrodes that showed a slight increase of Cr in the surrounding sediment, were not applied at lake scale. There were no complaints from the neighborhood (contrary, persons living at the lake showed great interest and supported the project), nor from authorities. Under-water movies made periodically document that the local fish (mostly perch) were attracted to the cathode and were frequently observed swarming it in big numbers. With our current state of knowledge, we deem the electrode technique safe.

5. Conclusions and Outlook

Immobilization of phosphate in lakes is feasible using sediment microbial fuel cells. This was documented both in laboratory microcosms and field experiments at Lake Søllerød in Denmark. The SMFCs were constructed from corrosion-resistant steel, which is easy to work with, widely available, low cost and a robust material. During the lake experiment over two seasons, little maintenance was needed. Although

the electricity produced by 16 m^2 of electrodes is low (10 mW), the environmental effects are more significant. Apart from reduced release of P from sediments, also methane and sulfide reduction, degradation of petroleum products and other organic pollutants and precipitation of some heavy metals seem feasible. The findings presented here thus open the way to novel and promising methods for sediment and lake restoration.

The study was designed as proof of concept. To upscale to a full-scale lake remediation, the kinetics of phosphate binding to sediments by SMFCs needs to be studied, in order to calculate the electrode area required for a satisfying P reduction. Other topics not addressed in this study include methane elimination, effects on the microbial community, lake sediment redox changes, nitrogen speciation, and also optimal design and construction of SMFCs.

Acknowledgements

Funding: This work was supported by the Ministry of Environment and Food of Denmark, through the Technology Development and Demonstration Program (MUDP), within the project “Implementation of the bioelectrode-technology for the improvement of the surface water environment.” In particular, we thank Thomas Rützou from MUDP for his support. We would like to thank Anders Vernersen and ‘Lystfiskerforeningen’ who graciously allowed the regular use of their boat in the lake, and Inge Thorsgaard of Rudersdal municipality for collaboration and field research permits. We thank Lykke Bjærge Bamdali and Marie Braad Lund for support with the DNA extraction and data analysis. We also thank Erik Arvin for establishing the contact to Rudersdal commune and for his advice. We would also like to thank NIRAS for the possibility to collaborate in the ideation of the lake electrode design, and the good people living around the lake for letting us work in such lovely surroundings. Finally, we thank Bent Skov for sharing his time, equipment, expertise, and excellent company.

Competing interests: the authors have no competing interests to declare.

547

548 **References**

549 Algar, C.K., Howard, A., Ward, C., Wanger, G., 2020. Sediment microbial fuel cells as a barrier to sulfide
550 accumulation and their potential for sediment remediation beneath aquaculture pens. Scientific
551 Reports, 10(1), 1–12. https://doi.org/10.1038/s41598-020-70002-4

552 Bastviken, D., Cole, J., Pace, M., Tranvik, L., 2004. Methane emissions from lakes: Dependence of lake
553 characteristics, two regional assessments, and a global estimate. Global Biogeochemical Cycles,
554 18:GB4009, doi:10.1029/2004GB0022

555 Boström, B., Jansson, M. & Forsberg, C., 1982. Phosphorus release from lake sediments. Arch. Hydro-
556 biol. Ergeb. Limnol. 18, 5-59.

557 Caraco, N.F., Cole, J.J. & Likens, G.E., 1993. Sulfate control of phosphorus availability in lakes – a test
558 and reevaluation of Hasler and Einsele's model. Hydrobiologia 253, 275–280.

559 Carlton, R.G., Wetzel, R.G., 1988. Phosphorous flux from lake sediments effects of epipelic algal oxygen
560 production. Limnology and Oceanography 33(4/1), 562-570.

561 Choi, Y.-J., Mohamed, H. O., Park, S.-G., Al Mayyahi, R. B., Al-Dhaifallah, M., Rezk, H., … Chae, K.-J.,
562 2019. Electrophoretically fabricated nickel/nickel oxides as cost effective nanocatalysts for the
563 oxygen reduction reaction in air-cathode microbial fuel cell. International Journal of Hydrogen
564 Energy. https://doi.org/10.1016/j.ijhydene.2019.05.091

565 Danish EPA / Miljøstyrelsen, 2020. Basic Analysis for Water Area Plan 2021-2027 part 2 and 3 (Danish:
566 Basisanalyse for vandområdeplaner 2021-2027). ISBN: 978-87-7038-143-7. Version March 2020.
567 Available at: https://www2.mst.dk/Udgiv/publikationer/2019/12/978-87-7038-143-7.pdf, last
568 accessed 18th January 2021

569 Danish Environmental Ministry / Miljøministeriet, 2012. Nature restoration – clean water in the mill river
570 system (Danish: Naturgenopretning - Rent vand i Mølleå-systemet). Report November 2020
571 available at https://naturstyrelsen.dk/media/nst/Attachments/VVMMlle_endeligjuni2012.pdf

572 De Schamphelaire, L., Rabaey, K., Boeckx, P., Boon, N., Verstraete, W., 2008. Outlook for benefits of
573 sediment microbial fuel cells with two bio-electrodes. Microbial Biotechnology, 1(6), 446–462.
574 https://doi.org/10.1111/j.1751-7915.2008.00042.x

575 Duras, J., Hejzlar, J., 2001. The effect of outflow depth on phosphorus retention in a small hypertrophic
576 temperate reservoir with short hydraulic residence time. Int. Rev. Hydrobiol. 86, 585-601.

577 ECHA European Chemical Agency, 2020. Registration dossier: Nickel, Ecotoxicological Summary.
578 Available at https://echa:europa:eu/registration-dossier/-/registered-dossier/15544/6/1 Last
579 accessed 2nd November 2020

580 EEA European Environmental Agency, 2020. Change in urban waste water treatment in European
581 countries, 1990-2017. https://www.eea.europa.eu/data-and-maps/daviz/change-in-urban-waste-
582 water last accessed 21 August 2020.

583 ESPI Metals, 2020. Stainless Steel 316 - Alloy Composition. Avilable at
584 https://www.espimetals.com/index.php/technical-data/202-stainless-steel-316-alloy-composition last
585 accessed 2nd November 2020

586 Friedman, E.S., McPhillips, L.E., Werner, J.J., Poole, A.C., Ley, R.E., Walter, M.T., Angenent, L.T., 2016,
587 Methane emission in a specific riparian-zone sediment decreased with bioelectrochemical
588 manipulation and corresponded to the microbial community dynamics. Front. Microbiol. 6, article
589 1523, pg. 1-12. DOI: 10.3389/fmicb.2015.01523

590 Gensemer, R.W., Playle, R.C., 1999. The bioavailability and toxicity of aluminum in aquatic environments.
591 Critical Reviews in Environmental Science and Technology, 29(4), 315-450. DOI:
592 10.1080/10643389991259245

593 Giles, C. D., Isles, P. D. F., Manley, T., Xu, Y., Druschel, G. K., & Schroth, A. W. (2016). The mobility of
594 phosphorus, iron, and manganese through the sediment–water continuum of a shallow eutrophic
595 freshwater lake under stratified and mixed water-column conditions. *Biogeochemistry*, *127*(1), 15–
596 34. https://doi.org/10.1007/s10533-015-0144-x

597 Gomez, E., Fillit M., Ximenes, M.C., Picot, B., 1998. Phosphate mobility at the sediment-water interface of
598 a Mediterranean lagoon (Etang du Mejean), seasonal phosphate variation. Hydrobiologia 374,
599 203- 216

600 Gupta, S., Yadav, A., Verma, N., 2017. Simultaneous Cr(VI) reduction and bioelectricity generation using
601 microbial fuel cell based on alumina-nickel nanoparticles-dispersed carbon nanofiber electrode.
602 Chemical Engineering Journal, 307, 729–738. https://doi.org/10.1016/j.cej.2016.08.130

603 Hansen, J., Reitzel, K., Jensen, H.S., Andersen, F.Ø., 2003. Effects of aluminum, iron, oxygen and nitrate
604 additions on phosphorus release from the sediment of a Danish softwater. Hydrobiologia 492,
605 139–149.

606 Haxthausen, von, K., 2021. PhD Thesis defended at the Technical University of Denmark, May 2021. In
607 preparation.

608 Hosomi, M., Okada, M., & Sudo, R. (1982). Release of phosphorus from lake sediments. *Environment*
609 *International*, *7*(2), 93–98. https://doi.org/10.1016/0160-4120(82)90078-2

610 Hupfer, M., Lewandowski, J., 2008. Oxygen controls the phosphorus release from lake sediments – a
611 long-lasting paradigm in limnology. Internat. Rev. Hydrobiol. 93(4–5), 415–432.

612 Hvidt, C.B., 2016. Investigation of the amount of anthropogenic sediment. (Danish: *Notat: Screening for*
613 *sedimentfjernelse i Søllerød Sø og Vejlesø)*. Report for Rudersdal kommune, 2016.

614 Jensen, H.S., Andersen, F.O., 1992. Importance of temperature, nitrate, and pH for phosphate release
615 from aerobic sediments of four shallow lakes. Limnology and Oceanography 37(3), 577-589.

616 Jensen H.S., Kristensen, P., Skytthe, A., 1992. Iron:phosphorous ratio in surface sediment as an indicator
617 of phosphate release from aerobic sediments in shallow lakes. Hydrobiologica 235/236, 731-743.

618 Jensen, H., Nielsen, H., Jensen, M., 2009. Investigation of phosphorous, iron and aluminum in sediments
619 from Lake Søllerød and Lake Vejle April 2009. (Danish: *Undersøgelse af fosfor , jern og*
620 *aluminium i sedimentet fra Søllerød Sø og Vejle Sø april 2009*). Report for the EU LIFE-projekt :
621 Re-establishing a natural water flow level.

https://naturstyrelsen.dk/media/nst/Attachments/2009_12_sedimentundersgelseSllerdogVejleS.pdf Last accessed 29th November 2020. Final project report at https://naturstyrelsen.dk/media/nst/Attachments/2012_07_07_final_report_hj1.pdf

Jensen, H. J., Møller, C., 2015. Environmental Condition of Lake Søllerød 2014. (Danish: *Miljøtilstand i Søllerød Sø 2014).* Report by Grontmij for Rudersdal municipality.

Grontmij, 2012. Environmental restoration – clean water in the Mølleå system. (Danish: *Naturgenopretning - Rent vand i Mølleå-systemet).* Report by Grontmij for The Danish Nature Agency, northern zealand. Avilable at https://naturstyrelsen.dk/media/nst/8432546/Milj%C3%B8redeg%C3%B8relse.pdf, last accessed 26th January 2021

Jørgensen, B. B., Findlay, A. J., & Pellerin, A. (2019). The biogeochemical sulfur cycle of marine sediments. *Frontiers in Microbiology*, *10*(APR), 1–27. https://doi.org/10.3389/fmicb.2019.00849

Jørgensen, E., Gabriel, S., Boock, P., 2001. Sediment investigations at lake Vejle and Lake Søllerød November 2000. (Danish: *Sedimentundersøgelser i Vejlesø og Søllerød Sø, november 2000*. Hedeselskabet for Copenhagen municipality, p. 1–16.

Kaur, A., Boghani, H.C., Michie, I., Dinsdale, R.M., Guwy, A.J., Premier, G.C., 2014. Inhibition of methane production in microbial fuel cells: Operating strategies which select electrogens over methanogens. Bioresource Technology 173, 75–81.

Kubota, K., Watanabe, T., Maki, H., Kanaya, G., Higashi, H., Syutsubo, K., 2019. Operation of sediment microbial fuel cells in Tokyo Bay, an extremely eutrophicated coastal sea. Bioresource Technology Reports, 6(February), 39–45. https://doi.org/10.1016/j.biteb.2019.02.001

Lehtoranta, J., Pitkänen, H., 2003. Binding of phosphate in sediment accumulation areas of the eastern Gulf of Finland, Baltic Sea. Hydrobiologia 492:55–67.

Liu, S., Feng, X., Li, X., 2017. Bioelectrochemical approach for control of methane emission from wetlands. Bioresource Technology 241, 812–820.

647 Logan, B.E., Hamelers, B., Rozendal, R., Schröder, U., Keller, J., Freguia, S., Aelterman, P., Verstraete,
648 W., Rabaey, K. 2006. Microbial fuel cells: Methodology and technology, Environ. Sci. Technol.
649 40, 5181–5192. https://doi.org/10.1021/es0605016

650 Logan, B.E., 2008. Materials. In: Logan, B.E., Microbial Fuel Cells. Wiley, New York, pp. 61-84.
651 https://doi.org/10.1002/9780470258590

652 Marzocchi, U., Palma, E., Rosetti, S., Aulenta, F., Scoma, A., 2020. Parallel artificial and biological
653 electric circuits power petroleum decontamination: The case of snorkel and cable bacteria. Water
654 Research 173, 115520.

655 Matturro, B., Viggi, C. C., Aulenta, F., & Rossetti, S. (2017). Cable bacteria and the bioelectrochemical
656 Snorkel: The natural and engineered facets playing a role in hydrocarbons degradation in marine
657 sediments. *Frontiers in Microbiology*, *8*(MAY), 1–13. https://doi.org/10.3389/fmicb.2017.00952

658 McAuliffe, T.F., Lukatelich, R.J., McComb, A.J., Qiu, S., 1998. Nitrate applications to control phosphorus
659 release from sediments of a shallow eutrophic estuary: an experimental evaluation. Mar. Freshw.
660 Res. 49, 463-473.

661 Nicolaisen, H.D. 2018. Lake restoration with bioelectrodes. BSc thesis at the Technical University of
662 Denmark, Lyngby.

663 Nur, R., Bates, M.H., 1979. The effects of pH on the aluminum, iron and calcium phosphate fractions of
664 lake sediments. Wat. Res. 13, 813-815.

665 Reitzel, K., Hansen, J., Jensen, H.S., Andersen, F.Ø., Hansen, K.S., 2003. Testing aluminum addition as
666 a tool for lake restoration in shallow, eutrophic Lake Sønderby, Denmark. Hydrobiologia 506–509,
667 781–787.

668 Roden, E. E., & Edmonds, J. W. (1997). Phosphate mobilization in iron-rich anaerobic sediments:
669 Microbial Fe(III) oxide reduction versus iron-sulfide formation. *Archiv für Hydrobiologie*, *139*(3), 347–
670 378. https://doi.org/10.1127/archiv-hydrobiol/139/1997/347

671 Ryckelynck, N., Stecher, H. A., & Reimers, C. E. (2005). Understanding the anodic mechanism of a
672 seafloor fuel cell: Interactions between geochemistry and microbial activity. *Biogeochemistry*, *76*(1),
673 113–139. https://doi.org/10.1007/s10533-005-2671-3

674 Singer, F.D., 2016. Ecology in Action. Cambridge University Press, Cambridge

675 Stumm, W., Morgan, J.J., 1996. Aquatic Chemistry. John Wiley and Sons, New York, 3rd ed.

676 Sulu-Gambari, F., Seitaj, D., Meysman, F. J., Schauer, R., Polerecky, L., & Slomp, C. P. 2016. Cable
677 Bacteria Control Iron-Phosphorus Dynamics in Sediments of a Coastal Hypoxic Basin.
678 Environmental Science & Technology, 50(3), 1227-1233. doi:10.1021/acs.est.5b04369

679 Søndergaard, M., Jensen, J.P., Jeppesen, E., 2005. Seasonal response of nutrients to reduced
680 phosphorus loading in 12 Danish lakes. Freshwater Biology 50, 1605-1615.

681 Søndergaard, M., 2007. Nutrient dynamics in lakes – with emphasis on phosphorus, sediment and lake
682 restorations. Doctor's dissertation (DSc). National Environmental Research Institute, University of
683 Aarhus, Denmark. 276 pp.

684 Tammeorg, O., Nürnberg, G., Niemistö, J., Haldna, M., Horppila, J., 2020. Internal phosphorus loading
685 due to sediment anoxia in shallow areas: implications for lake aeration treatments. Aquatic
686 Sciences 82,54,1-10 https://doi.org/10.1007/s00027-020-00724-0

687 Tender, L. M., Reimers, C. E., Stecher, H. A., Holmes, D. E., Bond, D. R., Lowy, D. A., Pilobello, K.,
688 Fertig, S. J., & Lovley, D. R. (2002). Harnessing microbially generated power on the seafloor. *Nature*
689 *Biotechnology*, *20*(8), 821–825. https://doi.org/10.1038/nbt716

690 Touch, N., Hibino, T., Morimoto, Y., Kinjo, N., 2017. Relaxing the formation of hypoxic bottom water with
691 sediment microbial fuel cells. Environmental Technology (United Kingdom), 38(23), 3016–3025.
692 https://doi.org/10.1080/09593330.2017.1285965

693 Yang, Q., Zhao, H., Zhao, N., Ni, J., Gu, X. 2016. Enhanced phosphorus flux from overlying water to
694 sediment in a bioelectrochemical system. Bioresource Technology 216, 182-187.
695 http://dx.doi.org/10.1016/j.biortech.2016.05.074

696

697 **Figure captions presented together with the figure**

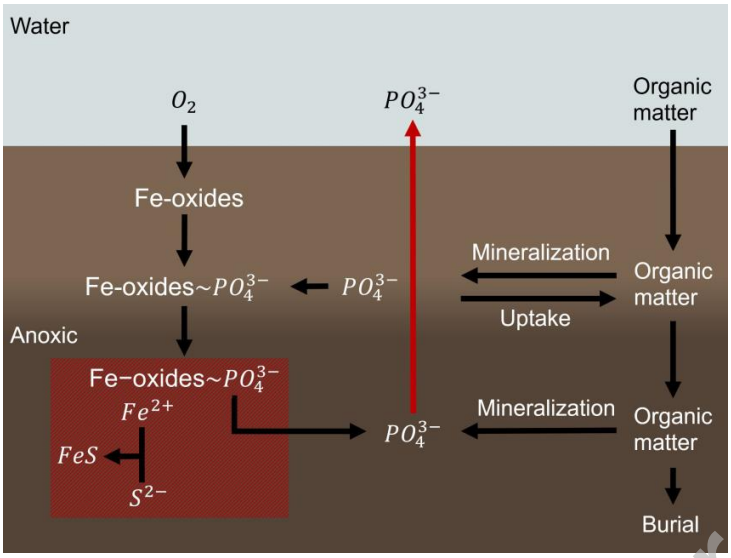

698

699 **Figure 1.** Postulated reactions. Mineralization of organic phosphorous deposited from the water to the
700 sediment produces phosphate (PO_4^{3-}). In oxic sediments matter, iron-oxides are present and bind
701 phosphate. In anoxic sediments (dark brown, bottom), Fe-oxides are reduced liberating Fe^{2+}, which in
702 turn, precipitates with sulfide (S^{2-}) as iron-sulfur minerals (FeS/FeS_2). This reduces the binding capacity of
703 the sediment towards phosphate, that may be then released to the water. By providing an alternative
704 electron sink, the anode of a SMFC inhibits the accumulation of S^{2-} and favors the reoxidation of Fe^{2+} to
705 Fe-oxides thereby maintaining an efficient binding mechanism for phosphate in the sediment (shown in
706 red shading).

707

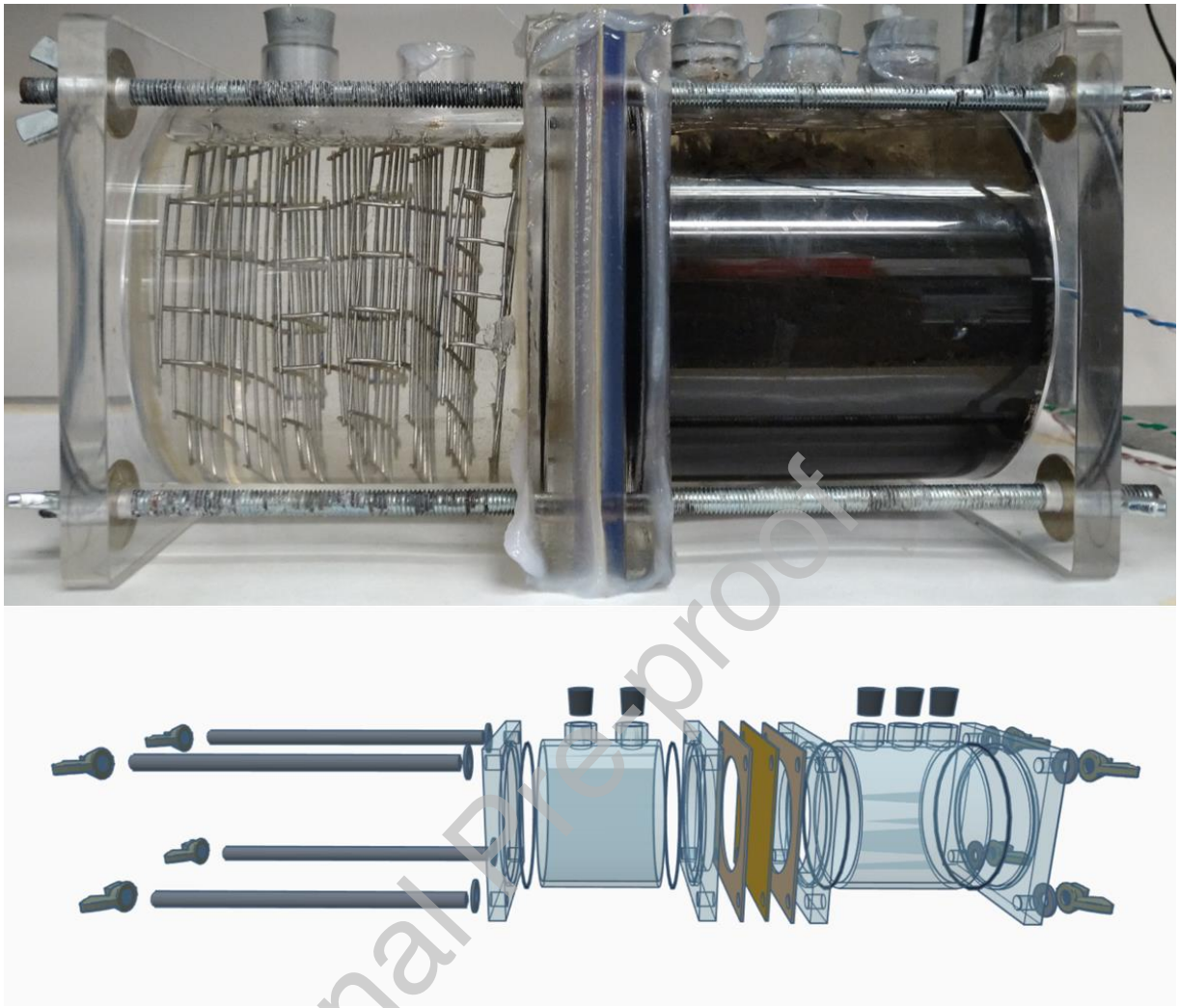

Figure 2. Laboratory microcosms (reactors). Top: operating microcosm containing lake water in the cathode chamber (left), and lake sediment and water in the anode chamber (right). Cathode and anode were made of stainless steel, folded to extend throughout their respective chambers. Bottom: external components of the microcosm. Elements left to right: wing nuts, tensioning rods, disk washers, end plate, O-ring, cathode chamber and stoppers, O-ring, interface plate, gasket, membrane, gasket, interface plate, O-ring, anode chamber and stoppers, end plate, washers, wingnuts.

716

717 **Figure 3.** Installation of electrodes in the lake. Anode was folded (A), electrodes were installed in frames
718 and towed in position (B). Electrodes were sunk. Cathode was suspended between surface buoys and
719 the anode on the bottom (C), performance was monitored by measuring working potential on shore (D).

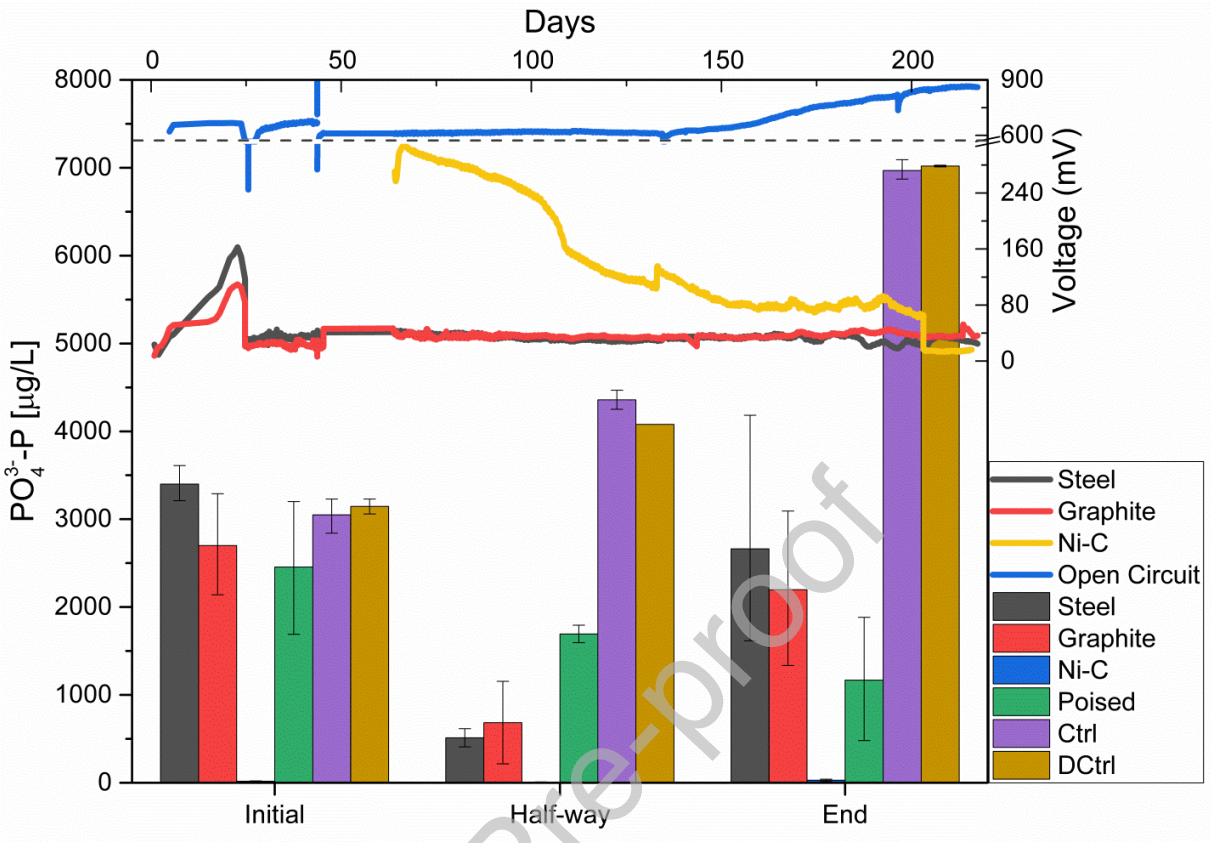

Figure 4. Results from lab scale experiment. Top: open circuit potential (OCP, mV, right axis), middle: working potentials (mV, right axis, mean of two replicates), below: dissolved phosphate in the water column PO_4-P (µg/L, left axis, error bars denote minimum and maximum, number of replicates n is 2 to 4) at initial (day 0), half-way (day 134) and the end (day 217). Electrode materials: stainless steel (Steel), stainless steel with addition of graphite particles (Graphite), stainless steel coated with carbon embedded with nickel particles (Ni-C), stainless steel with external voltage applied (Poised), no electrode (Ctrl), disconnected steel electrodes (DCtrl).

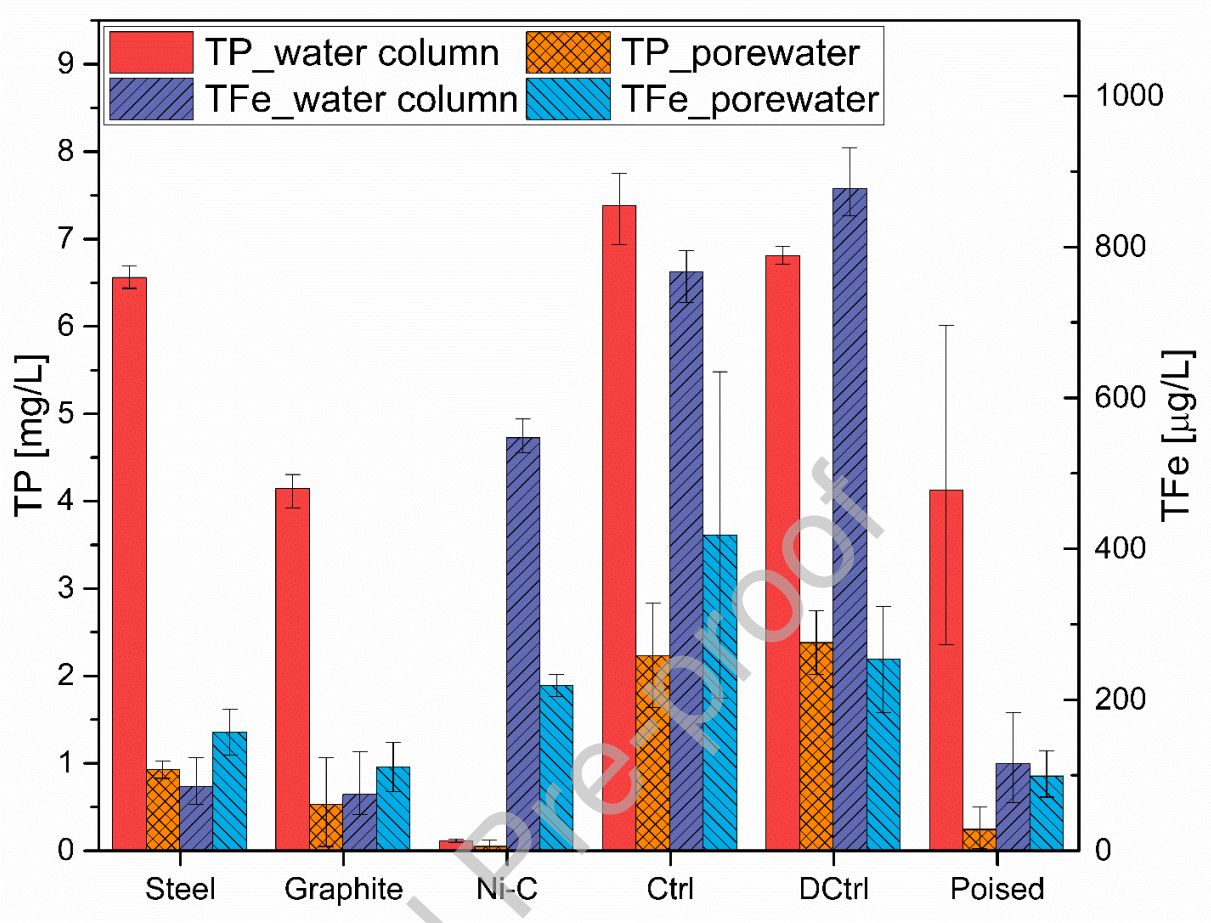

730

731 **Figure 5.** Total phosphorus (TP, mg/L, left axis) and total iron (TFe, µg/L, right axis) in sediment pore
732 water and in the water column of microcosms with and without sediment microbial fuel cells, at the
733 termination of the lab scale experiments on day 217. Error bars denote minimum to maximum, *n* is 2 to 6.
734 Electrode materials: stainless steel (Steel), stainless steel with addition of graphite particles (Graphite),
735 stainless steel coated with carbon embedded with nickel particles (Ni-C), stainless steel with external
736 voltage applied (Poised), no electrode (Ctrl), disconnected steel electrodes (DCtrl).

737

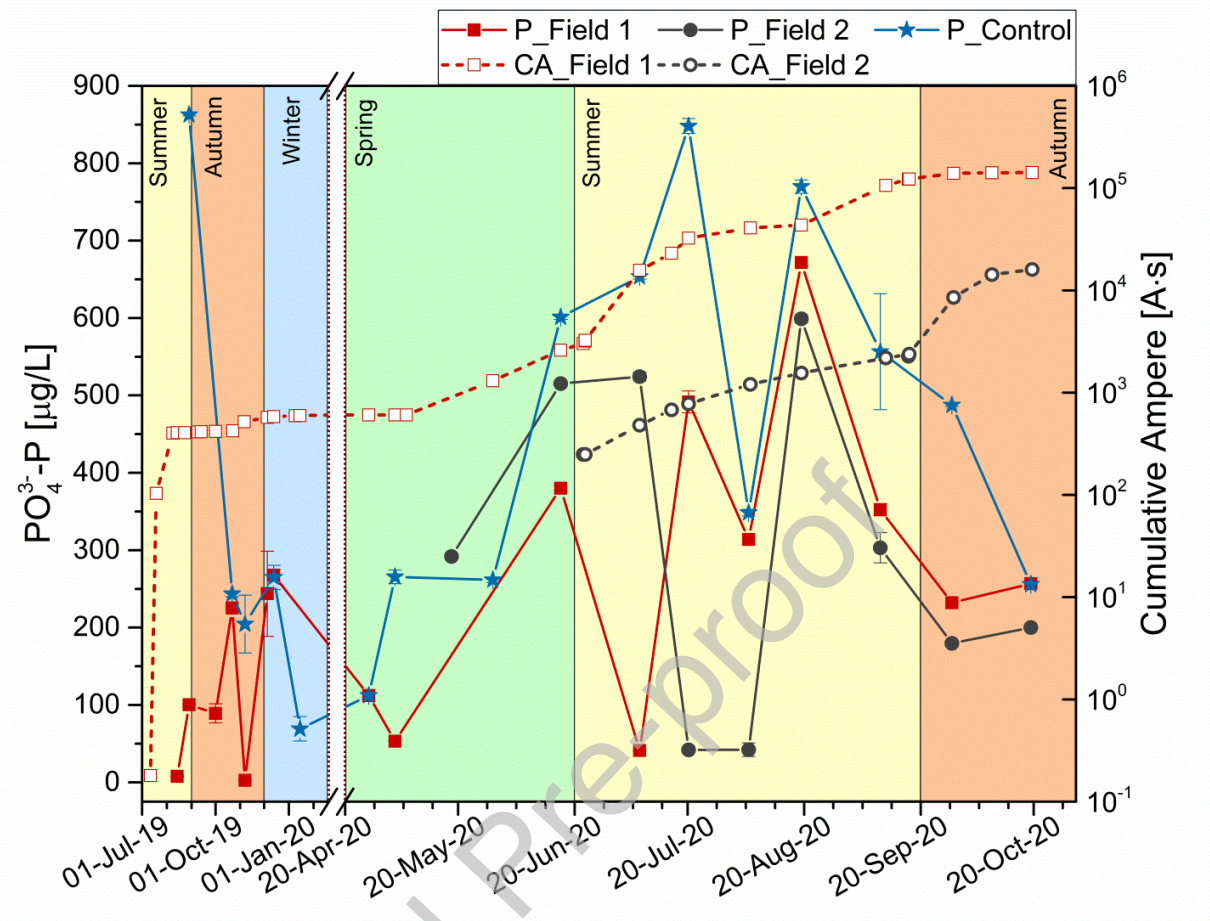

738

739 **Figure 6.** Lake scale sediment microbial fuel cell performance. Cumulative ampere (A·s) generated by the
740 electrodes of Field 1 and Field 2, and PO_4-P concentrations (µg/L) measured at the bottom of the lake
741 water column above the anodes and at a control site. Error bars denote standard deviation. The broken x-
742 axis between winter and spring corresponds to the time the cable to the anode in Field 1 was broken.

743

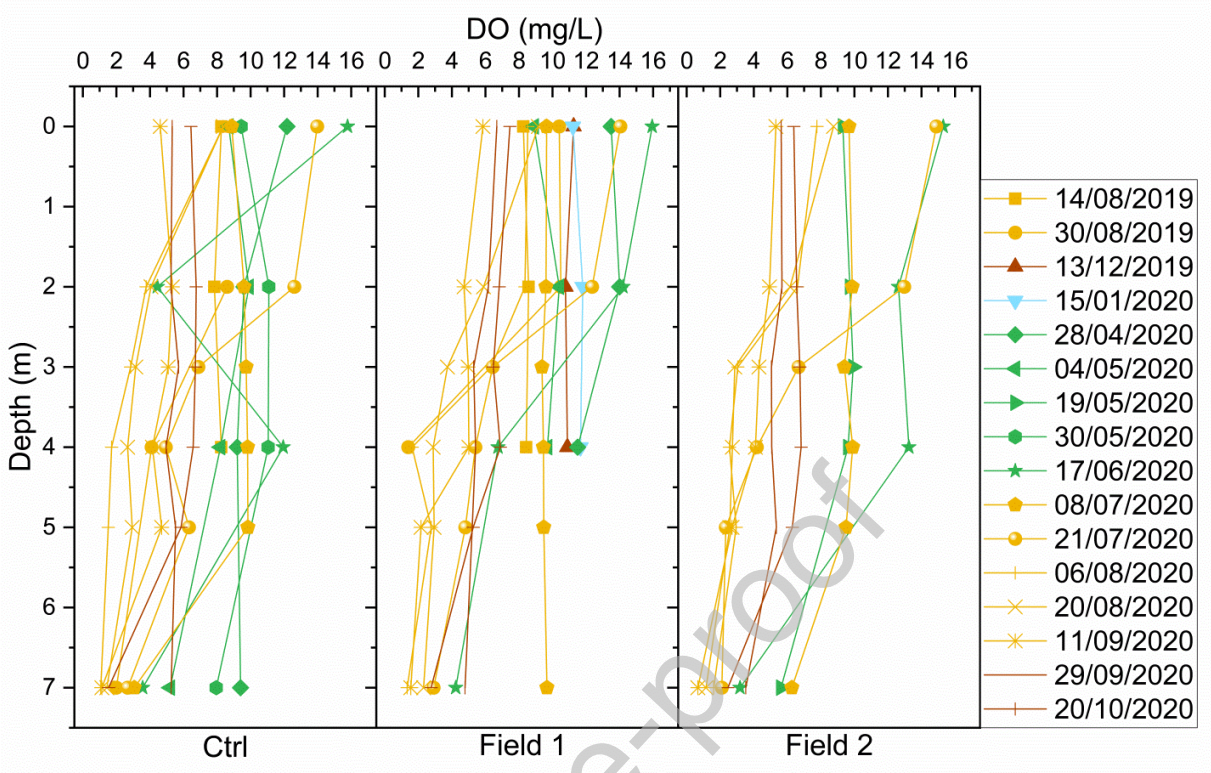

744 **Figure 7. Dissolved oxygen versus depth**. Dissolved oxygen (mg/L) measured in the lake water
745 column, within the SMFC fields and control area (Field 2 only from summer 2020). Green color is
746 sampling in spring, yellow in summer, red in autumn and blue in winter.